Global Change Biology

Global Change Biology (2016) **22**, 3750–3759, doi: 10.1111/gcb.13300

Limited effect of ozone reductions on the 20-year photosynthesis trend at Harvard forest

XU YUE[1,2], TREVOR F. KEENAN[3,4], WILLIAM MUNGER[5] and NADINE UNGER[1]

[1]*School of Forestry and Environmental Studies, Yale University, 195 Prospect Street, New Haven, CT 06511, USA,* [2]*Climate Change Research Center, Chinese Academy of Sciences, Beijing 100029, China,* [3]*Lawrence Berkeley National Lab, Berkeley, CA 94720, USA,* [4]*Department of Biological Sciences, Macquarie University, Sydney, NSW 2109, Australia,* [5]*Department of Earth and Planetary Sciences, School of Engineering and Applied Sciences, Harvard University, Cambridge, MA 02138, USA*

Abstract

Ozone (O_3) damage to leaves can reduce plant photosynthesis, which suggests that declines in ambient O_3 concentrations ($[O_3]$) in the United States may have helped increase gross primary production (GPP) in recent decades. Here, we assess the effect of long-term changes in ambient $[O_3]$ using 20 years of observations at Harvard forest. Using artificial neural networks, we found that the effect of the inclusion of $[O_3]$ as a predictor was slight, and independent of O_3 concentrations, which suggests limited high-frequency O_3 inhibition of GPP at this site. Simulations with a terrestrial biosphere model, however, suggest an average long-term O_3 inhibition of 10.4% for 1992–2011. A decline of $[O_3]$ over the measurement period resulted in moderate predicted GPP trends of 0.02–0.04 μmol C m^{-2} s^{-1} yr^{-1}, which is negligible relative to the total observed GPP trend of 0.41 μmol C m^{-2} s^{-1} yr^{-1}. A similar conclusion is achieved with the widely used AOT40 metric. Combined, our results suggest that ozone reductions at Harvard forest are unlikely to have had a large impact on the photosynthesis trend over the past 20 years. Such limited effects are mainly related to the slow responses of photosynthesis to changes in $[O_3]$. Furthermore, we estimate that 40% of photosynthesis happens in the shade, where stomatal conductance and thus $[O_3]$ deposition is lower than for sunlit leaves. This portion of GPP remains unaffected by $[O_3]$, thus helping to buffer the changes of total photosynthesis due to varied $[O_3]$. Our analyses suggest that current ozone reductions, although significant, cannot substantially alleviate the damages to forest ecosystems.

Keywords: artificial neural networks, decadal trend, deciduous forest, gross primary production, ozone inhibition, photosynthesis, stomatal conductance, terrestrial biosphere model

Received 1 February 2016; revised version received 18 March 2016 and accepted 25 March 2016

Introduction

Forests are important sinks for the terrestrial carbon cycle (Pan *et al.*, 2011). For example, North American ecosystems, mainly forests, absorb roughly 35% of the continental CO_2 emissions from fossil fuels (King *et al.*, 2012). Forest gross primary production (GPP) is sensitive to environmental factors, such as temperature, radiation, precipitation, and soil moisture (Beer *et al.*, 2010). In the recent decades, an increasing trend in the forest GPP and net ecosystem exchange of CO_2 (NEE) has been observed in the United States (Keenan *et al.*, 2013). Meteorological factors alone do not explain the decadal trend (Keenan *et al.*, 2012), although they significantly contribute to GPP variability on daily, seasonal, and interannual time scales.

Changes in tropospheric ozone concentrations could potentially contribute to the long-term trend and explain model discrepancies (Holmes, 2014; Keenan *et al.*, 2014). Tropospheric ozone (O_3) is a secondary air pollutant generated from the photochemical oxidation of carbon monoxide, methane, and volatile organic compounds by the hydroxyl radical in the presence of nitrogen oxides. Excessive O_3 exposure may damage plant photosynthesis and reduce terrestrial carbon sequestration (Sitch *et al.*, 2007). O_3 concentrations ($[O_3]$) in the United States have decreased significantly in the past decades due to emission regulation (Lefohn *et al.*, 2010), which could lead to increased forest GPP. Most field experiments examining O_3 damage are usually of short duration (e.g., references in Wittig *et al.*, 2007), which makes their extrapolation to long-term responses difficult. In recent decades, long-term continuous measurements of GPP and meteorological variables, such as temperature, radiation, and relative humidity have been measured using eddy covariance techniques at ecosystems around the world (Baldocchi, 2008). Among these sites, Harvard forest provides the longest record of observations (over 20 years) and has

Correspondence: Xu Yue, tel. +1 203 432 0773, fax +1 203 436 9135, e-mail: xu.yue@yale.edu

concurrent O_3 flux and concentration measurements (Wofsy *et al*., 1993; Horii *et al*., 2004). This long-term record provides a unique opportunity to examine the long-term effects of changes in $[O_3]$.

In this study, we explore the response of GPP to changes in O_3 concentrations at Harvard forest, taking advantage of the 1992–2011 simultaneous measurements of carbon fluxes, meteorological parameters, and atmospheric composition (Wofsy *et al*., 1993; Urbanski *et al*., 2007). We use two independent methods, including an artificial neural network (ANN), which is a widely used data-mining tool (Abramowitz, 2005), and the Yale Interactive terrestrial Biosphere (YIBs) model (Yue & Unger, 2014, 2015), which accounts for the influence of O_3 damage on photosynthesis (Sitch *et al*., 2007).

Materials and methods

Data

Long-term measurements are collected from the eddy covariance tower at the Harvard forest environmental measurement site (http://atmos.seas.harvard.edu/lab/hf/index.html) located in the New England region of the north-eastern United States (72.17°W, 42.54°N, elevation 340 m). The forest within the tower footprint is composed of red oak (*Quercus rubra*, 60% basal area), red maple (*Acer rubrum*, 23% basal area), and secondary deciduous species. We use hourly estimates of GPP, along with meteorological drivers, and atmospheric compositions from 1992 to 2011. GPP is derived from NEE by subtracting Reco (ecosystem respiration) that is computed from an exponential fit of nighttime NEE during well-mixed periods and air temperature (Urbanski *et al*., 2007). The meteorological variables include air temperature above the canopy (27 m), photosynthetically active radiation (PAR, 28 m), and relative humidity (RH) near surface (2.5 m). Data gaps are either filled with observations from nearby meteorological stations or interpolated based on the long-term mean diurnal cycles. Atmospheric $[CO_2]$ and $[O_3]$ are measured at eight vertical layers from 0.3 to 29 m. For this study, we use the values at the top of canopy (24.1 m), which are highly correlated with time series both below (18.3 m, $r = 0.98$) and above (29 m, $r = 0.99$) the canopy. The complete time series of these measurements are shown in Fig. S1. We focus our analysis on summer (June–July–August), when LAI is relatively constant, to exclude the phenological impacts on GPP (Richardson *et al*., 2009).

Artificial neural networks (ANN)

The ANN is a machine learning approach based on statistical multivariate modeling (Bishop, 1995). It is a powerful tool to identify the principle patterns underlying large sets of measurements, without prior assumptions about the relations between the targeted variables and various drivers. The ANN models have been widely used in the terrestrial biosphere and land surface studies and often outperform some semiempirical and process-based models (Abramowitz, 2005; Moffat *et al*., 2010). However, with a feed-forward ANN ensemble, Keenan *et al*. (2012) failed to predict the trend in the GPP at the Harvard forest for the complete period (1992–2009). In this study, we revisit this issue by training ANNs for each individual year and including $[O_3]$ as an additional predictor.

We develop two groups of ANN ensembles, each of which is trained with hourly or daily data. Each group includes four ANN models, driven with different combinations of meteorological variables (Table 1), so as to isolate the contribution of O_3 effect and compare it with other forcings. ANN_1 uses only temperature and PAR. ANN_2 uses RH, surface pressure, and wind speed, in addition to temperature and PAR. ANN_3 is the same as ANN_2 but adds $[CO_2]$. ANN_4 includes all the variables in ANN_3 as well as $[O_3]$. For each model, we train ANNs year by year for summer daytime, so as to exclude the possible impacts of interannual variations in both biotic (e.g., phenology and physiology) and abiotic (e.g., disturbance and nitrogen deposition) parameters on the GPP trend. As a result, we achieve 20 ANN models for each ensemble. We combine them to form a 20-year time series for evaluation. We exclude the hours or the days for a specific year if missing data account for >70% of the total moment. We calculate the R^2,

Table 1 Descriptions and statistics* for the ANN ensembles

Simulations	ANN_1	ANN_2	ANN_3	ANN_4
Inputs†	T, PAR	T, PAR, RH, PS, W	T, PAR, RH, PS, W, $[CO_2]$	T, PAR, RH, PS, W, $[CO_2]$, $[O_3]$
R^2	0.73 (0.48)	0.81 (0.53)	0.82 (0.59)	0.84 (0.62)
RMSE	4.94 (4.37)	4.20 (4.20)	4.01 (3.97)	3.85 (3.76)
Mean‡	19.0 (18.8)	18.9 (19.5)	18.7 (19.2)	18.8 (18.9)
Trend‡	0.45 (0.40)	0.43 (0.39)	0.41 (0.42)	0.41 (0.35)

*Statistics are performed at the same hours (8926 in total) when all model outputs are available. The values in brackets are calculated for ANN models trained with daily data.

†The inputs include temperature (*T*), photosynthetically active radiation (PAR), surface relative humidity (RH), surface pressure (PS), surface wind speed (W), carbon dioxide concentrations ($[CO_2]$), and ozone concentrations ($[O_3]$).

‡June–August daytime (6:00–20:00) averages (μmol C m^{-2} s^{-1}) and trends (μmol C m^{-2} s^{-1} yr^{-1}) during 1992–2012. The values are calculated at hours when all forcing variables are available.

root-mean-square error [RMSE, Eqn (1)], mean, and trend of the predictions to investigate how the inclusion of O_3 effects improves the ANN predictability and how it contributes to the long-term trend of GPP.

$$\mathrm{RMSE} = \sqrt{\frac{1}{N}\sum_{i=1}^{N}(P_i - O_i)^2} \quad (1)$$

Here, P_i and O_i are the pairs of predictions and observations, and N is the total records.

Yale Interactive terrestrial Biosphere (YIBs) model

The YIBs model is a process-based terrestrial biosphere model that simulates land carbon fluxes and dynamic tree growth (Yue & Unger, 2015). The model calculates leaf-level photosynthesis using the well-established Farquhar *et al.* (1980) scheme and the stomatal conductance model of Ball and Berry (Ball *et al.*, 1987). Leaf photosynthesis is integrated over multiple (typically 2–16 based on the convergence errors) canopy layers for both sun-lit and sun-shaded leaves to generate GPP (Unger *et al.*, 2013). A semimechanistic O_3 damage scheme (Sitch *et al.*, 2007), including a range of damage from low to high sensitivity, is implemented into the model (Yue & Unger, 2014). We use the same photosynthetic and allometric parameters for deciduous broadleaf forest (DBF) as indicated in Yue & Unger (2015). For example, the maximum carboxylation capacity (V_{cmax}) at 25 °C is set to 45 μmol m^{-2} s^{-1}, a value that results in the minimum RMSE between observations and the O_3-free simulations with YIBs at multiple DBF sites (Fig. S2). Precipitation is not a standard input for the YIBs model. Instead, the model considers the impacts of soil moisture, adopted from the ERA-interim reanalysis (http://www.ecmwf.int/), on ecosystem physiological processes, such as photosynthesis, stomatal conductance, phenology, and soil respiration (Yue & Unger, 2015).

We perform two-step simulations with the YIBs model. First, we evaluate the predicted O_3 damages for deciduous trees with measurements from the literature (Table 2). To do this, we apply fixed $[O_3]$ at 20 selected DBF sites (Table S1) from the FLUXNET network (http://fluxnet.ornl.gov) and the North American Carbon Program (Schaefer *et al.*, 2012). Harvard forest is also included in the network but its records span only for 1991–2006. For each site, we first run the YIBs model for an O_3-free simulation using the hourly measurements of $[CO_2]$ and meteorological variables (e.g., surface air temperature, relative humidity, wind speed, and shortwave radiation). We then perform two groups of sensitivity simulations, seven in each with fixed $[O_3]$ at 20, 40, 60, 80, 100, 120, 140 ppbv, respectively, using either high or low O_3 damages (Table 2). For the same level of $[O_3]$, the scheme from Sitch *et al.* (2007) considers a range of damage from low to high with corresponding sensitivity coefficients. We do not include seasonal and diurnal variations in $[O_3]$ for these sensitivity runs because most field experiments apply a constant level of $[O_3]$ during the test period (e.g., Feng *et al.*, 2008; Pellegrini *et al.*, 2011). All simulations (a total of 300) are run for the period when site-level records are available (Table S1). We compare the O_3-affected GPP from sensitivity simulations with O_3-free GPP from the control simulation and derive the O_3 damage percentages in GPP, which are compared with values from an ensemble of literatures (Table S2). Most of these field experiments are performed for tree species abundant at Harvard forest, such as oak and maple.

Table 2 Summary of sensitivity tests with the Yale Interactive terrestrial Biosphere vegetation model at 20 DBF sites

ID	Simulations*	$[O_3]$ (ppbv)	O_3 damage†
1	DBF_000	0	Null
2	DBF_020L	20	Low
3	DBF_020H	20	High
4	DBF_040L	40	Low
5	DBF_040H	40	High
6	DBF_060L	60	Low
7	DBF_060H	60	High
8	DBF_080L	80	Low
9	DBF_080H	80	High
10	DBF_100L	100	Low
11	DBF_100H	100	High
12	DBF_120L	120	Low
13	DBF_120H	120	High
14	DBF_140L	140	Low
15	DBF_140H	140	High

*Each simulation includes 20 separate runs at selected DBF sites (Table S1).

†Ozone damage applied in the simulation can be zero, low, or high for the same level of $[O_3]$, depending on the selection of damaging coefficients.

Second, we rerun the YIBs model at Harvard forest using time-varied $[O_3]$, $[CO_2]$, and meteorology for 1992–2011 (Table 3). We gap-fill the meteorological forcings using the Global Modeling and Assimilation Office (GMAO) Modern Era-Retrospective Analysis (MERRA) land product (Reichle *et al.*, 2011), which is interpolated to the site level based on the location of Harvard forest. We gap-fill $[CO_2]$ and $[O_3]$ with two steps: (i) We derive missing $[CO_2]$ or $[O_3]$ with the long-term regressions for each hour of the year developed using available samples at the same hour in the 20 years; and (ii) we fill the missing values using the average of the nearest 2 h.

For Harvard forest, we perform three groups (a total of 11) of simulations, each of which uses low (LO3), high (HO3), or null (NO3) O_3 damage sensitivity (Table 3). In the first two groups, eight sensitivity tests are designed to identify contributions of different forcings to the GPP trends. The ALL simulation is forced with the hourly meteorology, $[CO_2]$, and $[O_3]$ for 1992–2011. The MET simulation also uses year-to-year meteorology, but prescribed $[CO_2]$ and $[O_3]$ at the year 1992. The CO_2 simulation is forced with real time $[CO_2]$ but prescribed $[O_3]$ and recycled meteorology at the year 1992. The O_3 simulation follows the same strategy as the CO_2 simulation but with varied $[O_3]$ and fixed $[CO_2]$ at the year 1992. In addition to these eight runs, a reference simulation, named ALL_NO3, is forced with year-to-year meteorology and $[CO_2]$ but without O_3 damage. The final two simulations, OFF_LO3 and OFF_HO3, have the same configurations as that of

Table 3 Summary of simulations with the Yale Interactive terrestrial Biosphere vegetation model at Harvard forest

ID	Simulations	Meteorology	$[CO_2]$	$[O_3]$	O_3 damage
1	ALL_LO3	1992–2011	1992–2011	1992–2011	Low
2	MET_LO3	1992–2011	1992	1992	Low
3	CO2_LO3	1992	1992–2011	1992	Low
4	O3_LO3	1992	1992	1992–2011	Low
5	ALL_HO3	1992–2011	1992–2011	1992–2011	High
6	MET_HO3	1992–2011	1992	1992	High
7	CO2_HO3	1992	1992–2011	1992	High
8	O3_HO3	1992	1992	1992–2011	High
9	ALL_NO3	1992–2011	1992–2011	N/A	Null
10	OFF_LO3*	1992–2011	1992–2011	N/A	Null
11	OFF_HO3†	1992–2011	1992–2011	N/A	Null

*OFF_LO3 has the same configuration as that of ALL_NO3 but calculate offline O_3 vegetation damage with low sensitivity.
†OFF_HO3 has the same configuration as that of ALL_NO3 but calculate offline O_3 vegetation damage with high sensitivity.

ALL_NO3 but with offline calculations of O_3 damage with low and high sensitivities, respectively. Three additional 92-year (1900–1991) spin-up runs, using low, high, or null O_3 damage sensitivity, are initialized with tree height of 17.8 m and forced with recycled meteorology and prescribed $[CO_2]$ and $[O_3]$ at the year 1992 to reach equilibrium tree height. By the end of spin-up period, the predicted tree height is 17.6 m for the LO3 run, 16.9 m for the HO3 run, and 18.0 m for the NO3 run. The correspondent summer LAI is 4.02 m^2 m^{-2} for LO3 and 3.77 m^2 m^{-2} for HO3. Relative to the baseline simulation without O_3 damage, the LAI is reduced by 3.4% with low O_3 sensitivity and 9.3% with high O_3 sensitivity. Such differences reflect the steady-state effect of 100 model years of chronic O_3 exposure at the present-day pollution level. This long-term damage results from the weakened carbon pool for allocation processes and is different from the observed leaf injury caused by O_3 (Wan *et al.*, 2014).

Results

Evaluation of YIBs model and O_3 damage scheme

We validate the simulated carbon fluxes and O_3 damages from the YIBs model. The vegetation model successfully reproduces the magnitude and seasonality of GPP at most DBF sites globally (Fig. S2). The simulation at Harvard forest (US-Ha1) shows a relative bias of only −1% and a correlation coefficient up to 0.99 compared to the observations averaged for 1991–2006. Compared to measurements, the predicted mean O_3 damages at the 20 DBF sites show similar variations in response to the changes of $[O_3]$ (Fig. 1). In general, the increase of $[O_3]$ promotes the damages to both photosynthesis and stomatal conductance. The Sitch *et al.* (2007) scheme assumes the same O_3 damage levels to photosynthesis and stomatal conductance. Predicted damages in photosynthesis show high correlation coefficient of 0.6 with observed (Fig. 1c), while those in stomatal conductance have low correlations (Fig. 1d), suggesting that these two damages may be decoupled (Lombardozzi *et al.*, 2013). Such decoupling may be related to the sluggish responses of stomatal conductance (Hoshika *et al.*, 2015), but may also caused by the large uncertainties in the species-specific responses of stoma (Fig. 1b, d). On average, the observed damages are −21.1% for photosynthesis and −19.7% for stomatal conductance, both of which is consistent with the prediction of −20.7%.

Trends in observations at Harvard forest

The daytime GPP at Harvard forest increases significantly by 0.41 μmol m^{-2} s^{-1} yr^{-1} during 1992–2011 (Fig. 2). Nevertheless, meteorological fields show deviated trends at the same time. Temperature increases moderately by 0.02 °C yr^{-1} and PAR increases by 0.71 W m^{-2} yr^{-1}. A drier tendency is observed with a significant reduction of 0.32% yr^{-1} in RH. Meanwhile, atmospheric components exhibit significant ($P < 0.05$) changes as $[CO_2]$ increases by 1.76 ppm yr^{-1} and $[O_3]$ decreases by 0.46 ppb yr^{-1}. Gap-filled $[O_3]$ and $[CO_2]$ show similar trends, −0.49 ppb yr^{-1} for $[O_3]$ and 1.80 ppm yr^{-1} for $[CO_2]$, as the original data.

Detection of high-frequency O_3 damages with ANN

Using temperature and PAR alone, the ANN explains 73% (48% for ANNs trained with daily data) of the variance in GPP (Table 1). Additional drivers, such as RH, surface pressure, and wind speed, increase R^2 to 0.81 (0.53 for daily). A further but limited improvement (R^2 = 0.82 for hourly and 0.59 for daily) is achieved when adding $[CO_2]$ in the ANN models. Inclusion of $[O_3]$ has also very slight impacts, which moderately increase R^2 to 0.84 (0.62 for daily). The RMSE decreases gradually as the number of drivers used in the ANNs

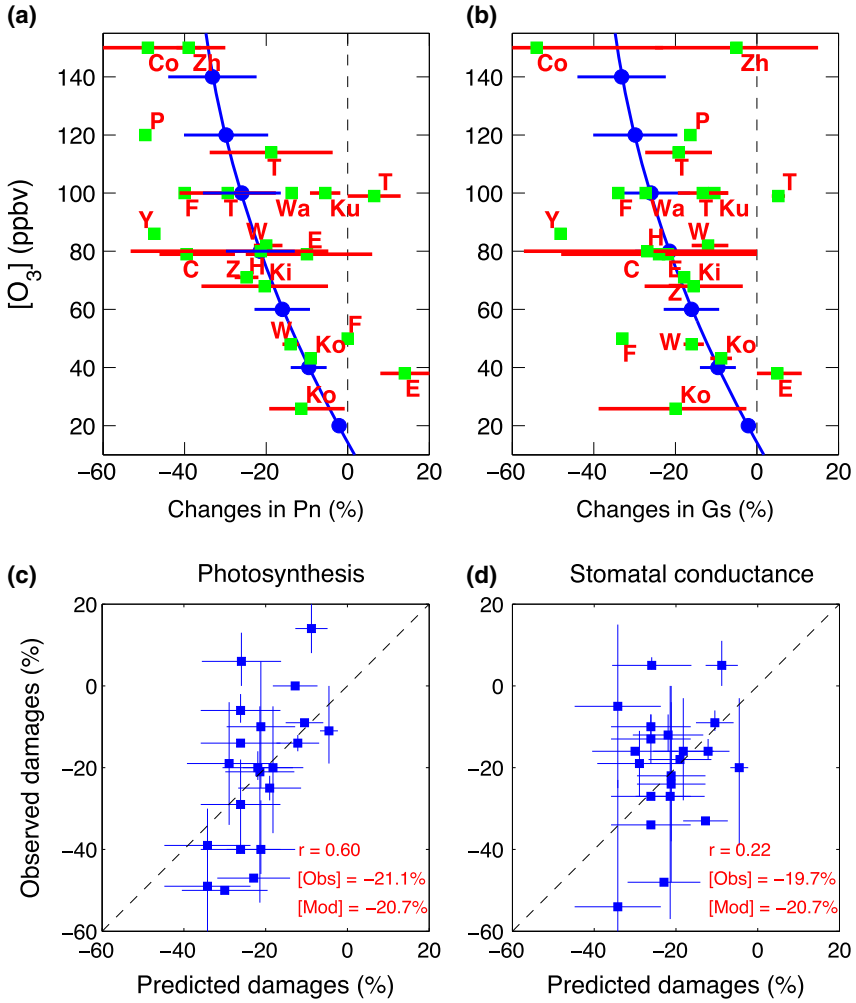

Fig. 1 Percentage changes in (a) photosynthesis and (b) stomatal conductance averaged across 20 deciduous broadleaf forest flux tower sites (see Table S1) in response to different levels of $[O_3]$ as simulated by the offline Yale Interactive terrestrial Biosphere model. Each simulation is performed with observed meteorology and $[CO_2]$ but fixed $[O_3]$ (Table 2). The horizontal blue lines show the damages ranging from low to high O_3 sensitivity, with the central blue points indicating the average reductions. The green solid squares with red lines show the results (mean plus uncertainty) based on measurements reported by multiple literatures (see Table S2). The author initials are indicated for the corresponding studies. The two-order polynomial curve fittings are applied to the simulated values. The derived percentage changes (including uncertainties) based on the fits are plotted against observations for (c) photosynthesis and (d) stomatal conductance. The correlation coefficients (r), mean damages from observations and simulations are shown in red on the scatter plots.

increased. Inclusion of $[O_3]$ reduces the simulation-to-observation RMSE (Fig. 3); however, such reductions of biases show similar magnitude for almost all $[O_3]$ intervals, suggesting that the effect of O_3 damage is independent of variations of $[O_3]$. The ANN models including O_3 trends do not present stronger trends in GPP than that without O_3 (Table 1). These results suggest that high-frequency O_3 damage is limited at this site.

Detection of long-term O_3 damages with YIBs model

With the YIBs model, we estimate an average online O_3 inhibition of 1.7 μmol C m^{-2} s^{-1} (10.4%) at Harvard forest for 1992–2011 (Fig. S3). This damage effect includes the feedback of LAI, as ozone-induced reductions in LAI will further decrease the total carbon uptake of the ecosystem. In the offline simulations, which ignore ozone damages to LAI, O_3 reduces GPP by 1.5 μmol C m^{-2} s^{-1} (9.2%) on average, suggesting moderate impacts of LAI feedbacks. The predicted year-to-year reductions in GPP are not correlated with $[O_3]$ (r = 0.04, Fig. 2d), suggesting that changes in $[O_3]$ are more related to the nonstomatal variables and processes, such as dry deposition, temperature, drought, and emissions of biogenic volatile organic compounds (Fares *et al.*, 2010). The

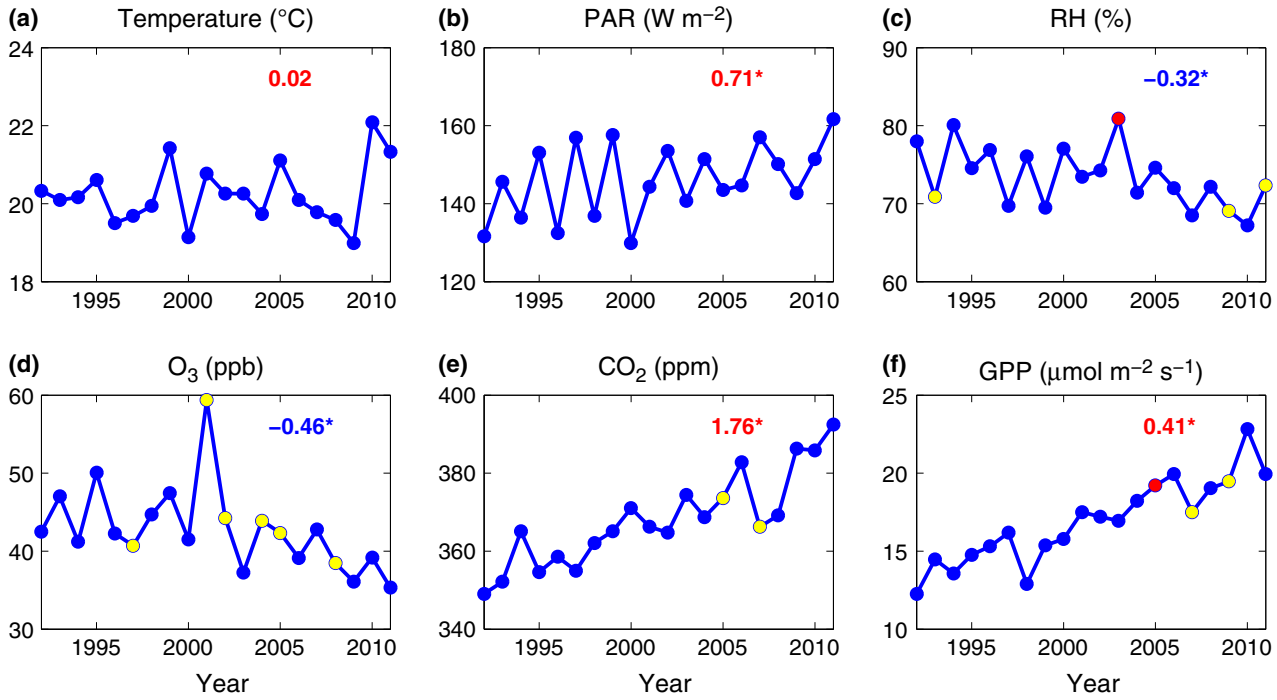

Fig. 2 Summer (June–August) daytime (6:00–20:00 local time) averages of (a) temperature, (b) photosynthetically active radiation (PAR), (c) relative humidity (RH), (d) ozone concentrations ($[O_3]$), (e) CO_2 concentrations ($[CO_2]$), and (f) gross primary production (GPP) at Harvard forest for 1992–2011. The point of a specific year is marked as yellow or red if the number of missing values account for >50% or >90% of the total records. Trends of time series, denoted on plots with red (blue) indicating positive (negative) values, are calculated by excluding those years with >50% missing values. Significant trends ($P < 0.05$) are denoted with asterisks. Trends of gap-filled $[O_3]$ and $[CO_2]$ are −0.49 ppb yr^{-1} and 1.80 ppm yr^{-1}, respectively.

semimechanistic scheme (Sitch *et al.*, 2007) calculates O_3 stomatal fluxes based on both ambient $[O_3]$ and stomatal conductance, the latter of which is closely related to GPP. The model predicts a long-term trend of ΔGPP of only 0.02 μmol C m^{-2} s^{-1} yr^{-1}, no matter whether the LAI feedbacks are included or not (Fig. S3). Driven with interannually varied meteorology, $[CO_2]$, and $[O_3]$, the model predicts a modest trend of 0.13 μmol C m^{-2} s^{-1} yr^{-1} (average of ALL_LO3 and ALL_HO3, Fig. 4), which is 67% lower than that of observations (Fig. 2f). Sensitivity tests with varied $[O_3]$ alone predict a trend of 0.03 μmol C m^{-2} s^{-1} yr^{-1} (average of ALL_LO3 and ALL_HO3), which accounts for only 7% of the observed, suggesting that the alleviation of O_3 pollution is not one of the primary contributors to the GPP trend at this forest. Other factors, such as meteorology and $[CO_2]$, also show limited contributions to the GPP trends relative to the observations, suggesting that other processes [such as a transition of forest composition hypothesized by Urbanski *et al.* (2007), which requires temporally varying model parameters (Keenan *et al.*, 2012)] are responsible for the long-term trends in GPP at Harvard forest.

Discussion

Causes of limited O_3 impacts on long-term GPP trends

Relative to 1992–1996, mean $[O_3]$ at Harvard forest decreases by 5.5 ppb (15%) during 2007–2011. Meanwhile, simulations with interannually varied $[O_3]$ alone predicts GPP increases only by 0.2–0.6 μmol C m^{-2} s^{-1} (2–4%, low to high sensitivity). Such unbalanced percentage changes in $[O_3]$ and GPP are mainly determined by the slow responses of photosynthesis to variations of $[O_3]$. According to the semimechanistic parameterization by Sitch *et al.* (2007), 5 ppb enhancement in $[O_3]$ on average induces additional damage of 1.6% in GPP (Fig. 1a). This response function is independent of the mechanistic schemes, such as that proposed by Sitch *et al.* (2007). As a comparison, we calculate the AOT40 [accumulated hourly (O_3) over a 40 ppb threshold], a metric to quantify O_3 damages used by many studies (e.g., Karlsson *et al.*, 2004), to reexamine the O_3-induced photosynthesis trend at Harvard forest. The summer daytime AOT40 at this site decreases by 0.49 ppm hour per year in the past 2 decades (Fig. S4). Based on the measurements from

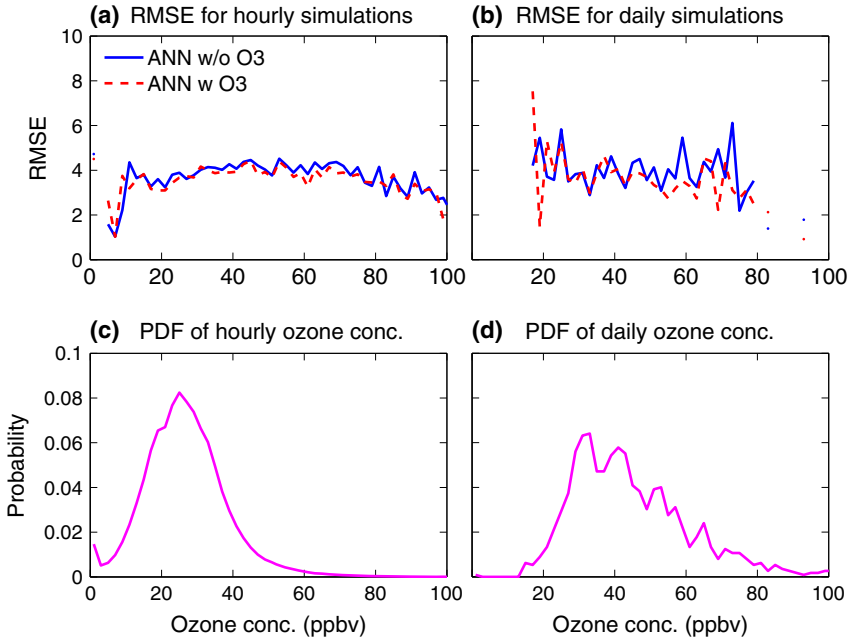

Fig. 3 Comparison of simulation-to-observation root-mean-square error (RMSE) for summer (a) hourly and (b) daily gross primary production (GPP) predicted by the artificial neural network (ANN) models with (red dashed) and without (blue solid) O_3. To calculate RMSE, we first sort and group GPP into 70 [O_3] bins from 0 to 140 ppbv. The RMSE in each [O_3] interval is then calculated based on the observed and simulated GPP in the same bin. The probability of summer daytime [O_3] is shown in (c) for hourly and (d) for daily O_3.

literatures (Table S2), we achieve an optimized response function of $F = -0.31 \times$ AOT40, where F is the percentage changes in photosynthesis (Fig. S5). As a result, the decreasing AOT40 increases GPP by 0.15% yr^{-1} (or 3% for the 20-year period), consistent with the estimates using the Sitch *et al.* (2007) scheme.

The unbalanced magnitudes of changes in [O_3] and GPP are also in part attributed to the buffering effects of stomatal conductance, which is not captured by the AOT40 metric. First, the decreasing rate of O_3 stomatal flux is lower than ambient [O_3]. Relative to the mean value in 1992–1996, canopy-level stomatal conductance is enhanced by 3.6 mmol m^{-2} s^{-1} (2%, with low ozone sensitivity) to 7.6 mmol m^{-2} s^{-1} (5%, with high ozone sensitivity) in 2007–2011. Such enhancement is related to the long-term increases of GPP and contributes to the increased efficiency of O_3 uptake. As a result, predicted O_3 stomatal flux at the same period decreases by 0.5–0.7 nmol m^{-2} s^{-1} (11–13%), less than that of ambient [O_3]. Second, a large fraction of GPP is not affected by the [O_3] reduction due to the low stomatal conductance of leaves. Experiments show oxidant tolerance from plant cells and tissues at low [O_3] (Ainsworth *et al.*, 2012). Observations also show no O_3 injury on shaded leaves (Wan *et al.*, 2014). In the model, O_3 inhibition is triggered only if the stomatal O_3 flux is higher than a specific threshold (1.6 nmol m^{-2} s^{-1} for deciduous trees) (Sitch *et al.*, 2007). To meet such threshold, both the ambient [O_3] and stomatal conductance is required to be above certain levels. However, 39% of the total carbon uptake is not affected by O_3, due to the fact that shaded leaves, which have low photosynthetic rates, have correspondingly low rates of stomatal conductance and thus low uptake of O_3. These leaves are usually at the lower canopy layers and/or shaded from sunlight. As a result, this portion of GPP remains relatively unaffected by [O_3], thus helping to buffer the changes in total carbon fluxes due to the varied [O_3].

Comparison with previous estimates

Our conclusion is not consistent with the estimate of Holmes (2014) (thereafter H2014) in which O_3 reduction significantly increases forest GPP. Both studies report a similar [O_3] reduction of 1.1% yr^{-1} in the north-eastern United States, but different trends in damaging metrics (flux-based for this study vs. exposure-based in H2014) and the GPP responses to these metrics. H2014 used AOT40 to estimate O_3 damage. At Harvard forest, AOT40 decreases by 4% yr^{-1} (absolute trend of −0.49 ppm h yr^{-1} divided by mean value of 11.9 ppm h for 1992–1996) during 1992–2011 (Fig. S4), which is much stronger than the trend of 0.8–1.0% yr^{-1} in stomatal O_3 flux estimated by this study. However, the AOT40 metric does not consider the buffering effects of stomatal conductance, for example, no O_3

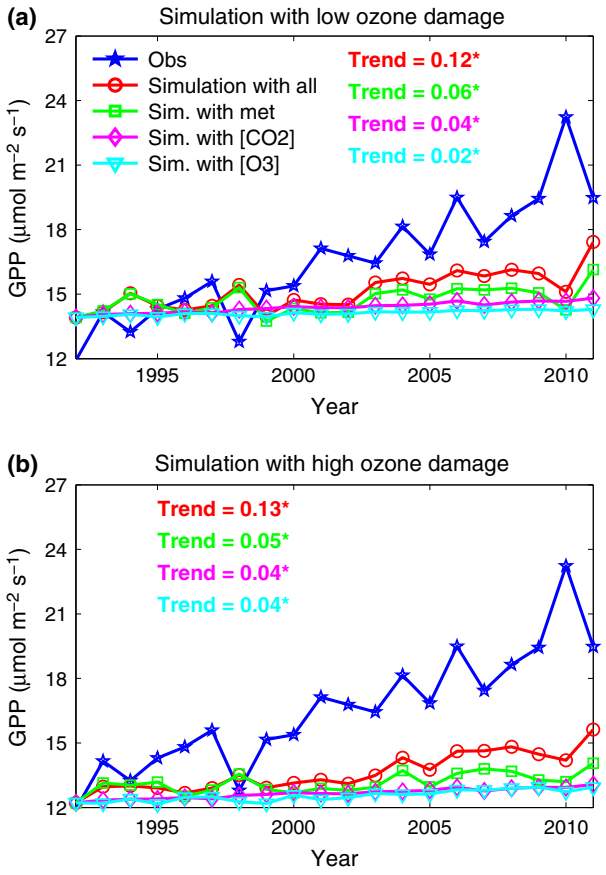

Fig. 4 Comparison of simulated summer daytime gross primary production (GPP) with observations (blue pentagram). Simulations are performed with Yale Interactive terrestrial Biosphere model using all varied forcings (red circle, ALL_LO3 and ALL_HO3), only varied meteorology (green square, MET_LO3 and MET_HO3), [CO_2] (magenta diamond, CO2_LO3 and CO2_HO3), and [O_3] (cyan triangle, O3_LO3 and O3_HO3). Trends of these simulations are shown with the same colors of lines. The descriptions of the abbreviations are summarized in Table 3. Units of trend are μmol C m^{-2} s^{-1} yr^{-1}.

injuries for shaded leaves (Wan *et al.*, 2014), thus overestimates the decreasing trend of O_3 damage. Furthermore, H2014 estimated GPP reduction based on the strong GPP responses to AOT40 as observed from the O_3 exposure experiment by Calatayud *et al.* (2007), who used young trees with height lower than 80 cm and applied open-top chambers that blow O_3 evenly in space and time. The response function of −0.7% per ppm hour derived by Calatayud *et al.* (2007) is much higher than the optimized value of −0.31% per ppm hour estimated based on multiple measurements (Table S2 and Fig. S5). Finally, the AOT40 metric is very uncertain because different studies may apply different definitions. For example, the AOT40 in Calatayud *et al.* (2007) was the cumulative [O_3] only for growth period (May to September), while H2014 calculated AOT40 for the whole year. No matter how AOT40 is defined, it is required to recalibrate the parameter a_0 in the response function $F = a_0 \times$ AOT40 based on the ensemble of measurements (Fig. S5).

Uncertainties

Estimate of O_3 damage is dependent on the reasonable responses of stoma. In this study, we apply the semimechanistic scheme proposed by Sitch *et al.* (2007), which assumes the same level of damages to stoma and photosynthesis caused by O_3. However, meta-analyses have shown that these two may have decoupled responses (Lombardozzi *et al.*, 2013). In addition, some measurements show that O_3 may lead to stomatal sluggishness (Hoshika *et al.*, 2015), which delays the stomatal responses to environmental stimuli. Here, we argue that the O_3 damages to stoma are (i) very uncertain and (ii) not affecting our main conclusion for photosynthesis trends. In another meta-analysis for trees, Wittig *et al.* (2007) summarized that elevation of O_3 on average depresses 11% in photosynthesis and 13% in stomatal conductance, suggesting these two have comparable responses to O_3 damages. In addition, the values taken from the literature (Table S2) show higher or equal damage rates in stomatal conductance compared with that in photosynthesis for 13 out 21 experiments. The average O_3-induced reductions in photosynthesis (−21%) and stomatal conductance (−20%) are also similar (Fig. 1). As a result, the decoupling responses and the stomatal sluggish might be species-specific and very uncertain. On the other hand, the application of calibrated AOT40 metric, which totally ignores any stomatal responses, achieves the same conclusion that O_3 reduction has limited impacts on photosynthesis trend, suggesting that stomatal responses might be the secondary driver. Finally, rising CO_2 may significantly decrease stomatal conductance (Keenan *et al.*, 2013), leading to reduced O_3 uptake. However, measurements show contrasting responses of stomatal acclimation to the long-term CO_2 change, suggesting that the elevated CO_2 may not alleviate O_3 uptake and the consequent damages (Paoletti & Grulke, 2005).

Other factors not accounted for here may further influence O_3-GPP relations. First, water availability influences both GPP and O_3 (White *et al.*, 2007; Ruehr *et al.*, 2012), and O_3-drought interactions may further decrease GPP (Sun *et al.*, 2012). We ignore these impacts and may underestimate O_3 inhibition rates in the relatively dry periods, although soil moisture is usually abundant at Harvard forest as indicated by the high RH (Fig. 2c). Second, many trees at Harvard forest emit isoprene, which protects plants from O_3 damage

(Loreto & Velikova, 2001). The current model does not include this mechanism and thus may actually overestimate O_3 damage at this site. Third, simulations with all forcings, including meteorology, [CO_2], and [O_3], cannot capture the observed GPP trend. Previous studies using data-fusion approach and/or other terrestrial models also report a similar inability to reproduce the observed trend at this site (Keenan *et al.*, 2012). Although we do not reproduce the observed trend of increasing GPP at Harvard forest, we show that reductions in [O_3] over recent decades are unlikely to contribute to the model-data mismatch.

Acknowledgements

Funding for this research was provided by Yale University. This project was supported in part by the facilities and staff of the Yale University Faculty of Arts and Sciences High Performance Computing Center. TFK acknowledges support from a Macquarie University research fellowship.

References

Abramowitz G (2005) Towards a benchmark for land surface models. *Geophysical Research Letters*, **32**, L22702.

Ainsworth EA, Yendrek CR, Sitch S, Collins WJ, Emberson LD (2012) The effects of tropospheric ozone on net primary productivity and implications for climate change. *Annual Review of Plant Biology*, **63**, 637–661.

Baldocchi D (2008) Breathing of the terrestrial biosphere: lessons learned from a global network of carbon dioxide flux measurement systems. *Australian Journal of Botany*, **56**, 1–26.

Ball JT, Woodrow IE, Berry JA (1987) A model predicting stomatal conductance and its contribution to the control of photosynthesis under different environmental conditions. In: *Progress in Photosynthesis Research* (ed. Biggins J), pp. 221–224. Nijhoff, Dordrecht, Netherlands.

Beer C, Reichstein M, Tomelleri E *et al.* (2010) Terrestrial gross carbon dioxide uptake: global distribution and covariation with climate. *Science*, **329**, 834–838.

Bishop CM (1995) *Neural Networks for Pattern Recognition*. Oxford University Press, Oxford, UK.

Calatayud V, Cervero J, Sanz MJ (2007) Foliar, physiological and growth responses of four maple species exposed to ozone. *Water Air and Soil Pollution*, **185**, 239–254.

Fares S, Mckay M, Holzinger R, Goldstein R (2010) Ozone fluxes in a *Pinus ponderosa* ecosystem are dominated by non-stomatal processes: evidence from long-term continuous measurements. *Agricultural and Forest Meteorology*, **150**, 420–431.

Farquhar GD, Caemmerer SV, Berry JA (1980) A biochemical-model of photosynthetic CO_2 assimilation in leaves of C-3 species. *Planta*, **149**, 78–90.

Feng ZZ, Zeng HQ, Wang XK, Zheng QW, Feng ZW (2008) Sensitivity of *Metasequoia glyptostroboides* to ozone stress. *Photosynthetica*, **46**, 463–465.

Holmes CD (2014) Air pollution and forest water use. *Nature*, **507**, E1–E2.

Horii CV, Munger JW, Wofsy SC, Zahniser M, Nelson D, Mcmanus JB (2004) Fluxes of nitrogen oxides over a temperate deciduous forest. *Journal of Geophysical Research*, **109**, D08305.

Hoshika Y, Katata G, Deushi M, Watanabe M, Koike T, Paoletti E (2015) Ozone-induced stomatal sluggishness changes carbon and water balance of temperate deciduous forests. *Scientific Reports*, **5**, 09871.

Karlsson PE, Uddling J, Braun S *et al.* (2004) New critical levels for ozone effects on young trees based on AOT40 and simulated cumulative leaf uptake of ozone. *Atmospheric Environment*, **38**, 2283–2294.

Keenan TF, Davidson E, Moffat AM, Munger W, Richardson AD (2012) Using model-data fusion to interpret past trends, and quantify uncertainties in future projections, of terrestrial ecosystem carbon cycling. *Global Change Biology*, **18**, 2555–2569.

Keenan TF, Hollinger DY, Bohrer G, Dragoni D, Munger JW, Schmid HP, Richardson AD (2013) Increase in forest water use efficiency as atmospheric CO_2 concentrations rise. *Nature*, **499**, 324–327.

Keenan TF, Hollinger DY, Bohrer G, Dragoni D, Munger JW, Schmid HP, Richardson AD (2014) Air pollution and forest water use reply. *Nature*, **507**, E2–E3.

King AW, Hayes DJ, Huntzinger DN, West TO, Post WM (2012) North American carbon dioxide sources and sinks: magnitude, attribution, and uncertainty. *Frontiers in Ecology and the Environment*, **10**, 512–519.

Lefohn AS, Shadwick D, Oltmans SJ (2010) Characterizing changes in surface ozone levels in metropolitan and rural areas in the United States for 1980–2008 and 1994–2008. *Atmospheric Environment*, **44**, 5199–5210.

Lombardozzi D, Sparks JP, Bonan G (2013) Integrating O_3 influences on terrestrial processes: photosynthetic and stomatal response data available for regional and global modeling. *Biogeosciences*, **10**, 6815–6831.

Loreto F, Velikova V (2001) Isoprene produced by leaves protects the photosynthetic apparatus against ozone damage, quenches ozone products, and reduces lipid peroxidation of cellular membranes. *Plant Physiology*, **127**, 1781–1787.

Moffat AM, Beckstein C, Churkina G, Mund M, Heimann M (2010) Characterization of ecosystem responses to climatic controls using artificial neural networks. *Global Change Biology*, **16**, 2737–2749.

Pan YD, Birdsey RA, Fang JY *et al.* (2011) A large and persistent carbon sink in the world's forests. *Science*, **333**, 988–993.

Paoletti E, Grulke NE (2005) Does living in elevated CO_2 ameliorate tree response to ozone? A review on stomatal responses. *Environmental Pollution*, **137**, 483–493.

Pellegrini E, Francini A, Lorenzini G, Nali C (2011) PSII photochemistry and carboxylation efficiency in *Liriodendron tulipifera* under ozone exposure. *Environmental and Experimental Botany*, **70**, 217–226.

Reichle RH, Koster RD, De Lannoy GJM, Forman BA, Liu Q, Mahanama SPP, Toure A (2011) Assessment and enhancement of MERRA land surface hydrology estimates. *Journal of Climate*, **24**, 6322–6338.

Richardson AD, Hollinger DY, Dail DB, Lee JT, Munger JW, O'keefe J (2009) Influence of spring phenology on seasonal and annual carbon balance in two contrasting New England forests. *Tree Physiology*, **29**, 321–331.

Ruehr NK, Martin JG, Law BE (2012) Effects of water availability on carbon and water exchange in a young ponderosa pine forest: above- and belowground responses. *Agricultural and Forest Meteorology*, **164**, 136–148.

Schaefer K, Schwalm CR, Williams C *et al.* (2012) A model-data comparison of gross primary productivity: results from the North American Carbon Program site synthesis. *Journal of Geophysical Research*, **117**, G03010.

Sitch S, Cox PM, Collins WJ, Huntingford C (2007) Indirect radiative forcing of climate change through ozone effects on the land-carbon sink. *Nature*, **448**, 791–794.

Sun G, Mclaughlin SB, Porter JH, Uddling J, Mulholland PJ, Adams MB, Pederson N (2012) Interactive influences of ozone and climate on streamflow of forested watersheds. *Global Change Biology*, **18**, 3395–3409.

Unger N, Harper K, Zheng Y *et al.* (2013) Photosynthesis-dependent isoprene emission from leaf to planet in a global carbon–chemistry–climate model. *Atmospheric Chemistry and Physics*, **13**, 10243–10269.

Urbanski S, Barford C, Wofsy S *et al.* (2007) Factors controlling CO_2 exchange on timescales from hourly to decadal at Harvard Forest. *Journal of Geophysical Research*, **112**, G02020.

Wan WX, Manning WJ, Wang XK, Zhang HX, Sun X, Zhang QQ (2014) Ozone and ozone injury on plants in and around Beijing, China. *Environmental Pollution*, **191**, 215–222.

White AB, Darby LS, Senff CJ *et al.* (2007) Comparing the impact of meteorological variability on surface ozone during the NEAQS (2002) and ICARTT (2004) field campaigns. *Journal of Geophysical Research*, **112**, D10s14.

Wittig VE, Ainsworth EA, Long SP (2007) To what extent do current and projected increases in surface ozone affect photosynthesis and stomatal conductance of trees? A meta-analytic review of the last 3 decades of experiments. *Plant Cell and Environment*, **30**, 1150–1162.

Wofsy SC, Goulden ML, Munger JW *et al.* (1993) Net exchange of CO_2 in a midlatitude forest. *Science*, **260**, 1314–1317.

Yue X, Unger N (2014) Ozone vegetation damage effects on gross primary productivity in the United States. *Atmospheric Chemistry and Physics*, **14**, 9137–9153.

Yue X, Unger N (2015) The Yale Interactive terrestrial Biosphere model: description, evaluation and implementation into NASA GISS ModelE2. *Geoscientific Model Development*, **8**, 2399–2417.

Supporting Information

Additional Supporting Information may be found in the online version of this article:

Table S1. Descriptions of 20 DBF flux tower sites from NACP and FLUXNET.
Table S2. Summary of measurements for ozone tree damages from literature.
Fig. S1. Hourly measurements of meteorology and gases at Harvard forest.
Fig. S2. Evaluation of simulated monthly GPP at 20 DBF sites.
Fig. S3. Predicted year-to-year ozone damage to GPP at Harvard forest.
Fig. S4. Changes of summer daytime AOT40 in the past 2 decades.
Fig. S5. Calibration of AOT40 metrics with literature-based measurements.